

Natural strontium isotope composition as a tracer of weathering patterns and of exchangeable calcium sources in acid leached soils developed on loess of central Belgium

TH. DROUET^a, J. HERBAUTS^a, W. GRUBER^a & D. DEMAIFFE^b

^aLaboratoire de Génétique et d'Ecologie Végétales, Université Libre de Bruxelles (ULB), 1850 chaussée de Wavre, B-1160 Bruxelles, and ^bLaboratoire de Géochimie Isotopique, Université Libre de Bruxelles (ULB), CP 160/02, 50 av. F.D. Roosevelt, B-1050 Bruxelles, Belgium

Summary

The natural Sr isotope composition of acid leached soils developed on loess, under beech forest, in central Belgium was used as a tracer of soil forming processes, in conjunction with physico-chemical and quantitative mineralogical investigations. Attention was focused on weathering and exchange processes, with special emphasis on the origin of the current soil exchangeable fraction and the influence of the atmospheric deposition and biological cycling on the calcium exchangeable pool (Sr acts as a proxy for Ca). The determination of $^{87}\text{Sr}/^{86}\text{Sr}$ ratios was made on the bulk soil, on the clay- and silt-size soil separates, on 0.1 M HCl extracts, on the labile pool, on the soil solution and on the bulk precipitation. The acid leached soil profiles are characterized by a sequence of weathering processes that is highlighted by both mineralogical and isotopic changes. From the calcareous unweathered loess (pH 7.5) to the uppermost soil horizons (pH < 4.0) the evolution of the $^{87}\text{Sr}/^{86}\text{Sr}$ isotope ratio clearly reflects: (i) the selective weathering of Ca-plagioclase (small $^{87}\text{Sr}/^{86}\text{Sr}$ ratio) and the increasing proportion of resistant K- and Rb-rich minerals (large $^{87}\text{Sr}/^{86}\text{Sr}$ ratio) in the uppermost soil horizons; and (ii) a downward translocation of clay minerals with a large isotopic ratio, a physical breakdown of muscovite and a non-congruent chemical weathering of K-feldspar. The influence of organic restitutions or atmospheric deposition is not significant. The comparison between the Sr isotopic signature of the soil solution, and the exchangeable and HCl-extractible soil fractions provides information about cation exchange efficiency, soil–water interaction and the origin of the exchangeable pool.

Introduction

Strontium isotopes are a powerful tool in ecosystem studies, both as a tracer of nutrient sources of forest stands (Graustein & Armstrong, 1983; Miller *et al.*, 1993; Bailey *et al.*, 1996; Blum *et al.*, 2002; Kennedy *et al.*, 2002; Poszwa *et al.*, 2004; Drouet *et al.*, 2005a), and as a monitor of weathering processes, mainly in catchment studies (Åberg *et al.*, 1989; Bain & Bacon, 1994; Clow *et al.*, 1997; Probst *et al.*, 2000), but also less frequently in the soil environment itself (Bullen *et al.*, 1997; Blum & Erel, 1997). All these studies imply knowledge of the Sr isotopic signature ($^{87}\text{Sr}/^{86}\text{Sr}$ ratio) of the main sources governing Sr fluxes in the soil-water-vegetation system, e.g. atmospheric inputs and mineral weathering release. The isotopic composition of

the mineral source (the weathering end-member) is, however, difficult to estimate given the mixing of several Sr-bearing minerals with distinct Sr isotope ratios and different weathering rates. In addition, in soils, minerals are unequally distributed with depth, owing to the fact that the mineralogical composition of most of the soil profiles is not only determined by the nature of the parent material, but also depends on soil forming processes that can lead to vertical mineralogical gradients.

Strontium, which is ubiquitous in nature and one of the most abundant of the trace elements in surficial deposits and rocks, acts as a proxy for Ca because both are alkaline earth elements with similar ionic radius and the same valence (Capo *et al.*, 1998). Consequently, Sr and Ca behave very similarly in the environment and hence, the natural Sr isotope system has been used to trace Ca sources and fluxes in forest ecosystems and to

Correspondence: T. Drouet. E-mail: tdrouetd@ulb.ac.be
Received 26 April 2005; revised version accepted 20 April 2006

calculate Ca weathering rates and budgets in catchment studies. Few Sr isotope studies, however, have been focused on the soil forming processes themselves.

The main objective of the present study is to determine which soil parameters explain the vertical distribution of the isotope composition of exchangeable and non-exchangeable Sr in forested acid leached soils (Dystric Podzoluvisols) developed in the loess belt of central Belgium. Special attention is focused on processes such as mineral weathering, clay-illuviation, cation exchange and biotic influences. To this end, Sr isotopic determinations were made in five soil profiles and compared with their physico-chemical characteristics and with the qualitative and quantitative distribution of minerals throughout the soil horizons. For two profiles, quantitative weathering patterns of the main soil minerals were determined using an isoelement assessment method (Lelong & Souchier, 1970; Sohet *et al.*, 1988; El Bayad, 1996). This provides the opportunity to trace the products from weathering of individual minerals, by knowing which minerals are present in the different soil horizons and in which proportions. Sr isotope measurements were made systematically on the bulk soil and on the exchangeable soil fraction. In one of the stands studied, Sr isotopic measurements were extended to the silt- and clay-size fractions, to the 0.1 M HCl extracts, which simulated natural weathering, and to soil water samples collected *in situ*. The aim is to determine more precisely which relations can be established between the Sr isotopic patterns of these different soil pools. Our view is that a better understanding of the behaviour of natural Sr isotopes in the soil environment will improve our knowledge of weathering and open new prospects on the dynamics of soil exchange processes.

Materials and methods

Site descriptions

Soils of five forest stands were selected for this study in the loess belt of central Belgium. All are located in the Soignes Regional Forest, southeast of Brussels (50°47'N, 4°27'E). This forest covers 4400 ha of a loessic plateau at about 120 m above sea level. The climate is of an Atlantic type, with an average annual rainfall of 780 mm and a mean annual temperature of 9.8°C. The natural vegetation is a deciduous forest with oak (*Quercus robur* L. and *Q. petraea* (Mattuschka) Lieblein) and European beech (*Fagus sylvatica* L.) as codominant species. However, beech has been planted extensively since the end of the 18th century and all the study sites are even-aged beech high forests. Most of them were planted between 1803 and 1865. The ground vegetation is dominated by moder-mor indicator species (*Pteridium aquilinum* (L.) Kuhn, *Deschampsia flexuosa* (L.) Trin., *Carex pilulifera* L. and *Polytrichum formosum* Hedw.), associated with acid mull indicators (*Milium effusum* L., *Oxalis acetosella* L. and *Dryopteris dilatata* (Hoffm.) A. Gray). Prevailing soils are acid leached soils with an A_hEB_hC soil profile (Dystric Podzoluvisols:

FAO-Unesco, 1975). These soils are acid and strongly desaturated to at least 1 m depth. The soil parent material is a Pleistocene aeolian loess deposit, several metres thick. In its upper metres, the loess is dated from the end of the Würm glaciation (Pleniglacial B: Brabantian loess, ~20 000 years BP; Haesaerts, 1985). Beneath the loess occur Tertiary marine sediments, mainly Eocene clayey sands. All the soils studied are developed in the loess deposit and therefore belong to the silt loam textural class. Morphological, chemical and mineralogical studies on similar forested soils of the Belgian loess belt were made by Van Ranst *et al.* (1982), El Bayad (1996) and Brahy *et al.* (2000).

Sampling

The main forest site studied is the *Mésanges* even-aged beech stand (hereafter MES). In this site, repeated soil samplings have been carried out since the 1980s for dendrochemical studies (Penninckx *et al.*, 1999; Drouet *et al.*, 2005b). Three complementary beech stands were selected for the present work in the Soignes Regional Forest, on similar loessial parent material and soil type (Dystric Podzoluvisols): *Tumuli*, *Tir aux pigeons* and *Relais des Dames* sites (hereafter TUM, PIG and REL II).

Soil samples were taken from soil pits (MES I, TUM) or by augering (MES II, PIG, REL II). Major soil horizons were systematically sampled: A_h (0–5 cm), E (5–25 cm), B_{21t} (55–75 cm) and B_{31t} (175–200 cm). The carbonated C_k horizon (the unweathered loess) was also sampled at the base of the niveo-aeolian deposit (> 250 cm). In the main MES site and in the TUM site, a more detailed sampling of soil profiles was made, covering 11 and 8 horizons or subhorizons, respectively.

The soil solution was collected *in situ*, using a soil moisture sampling system with tension water samplers (Teflon/quartz porous probes, PRENART equipment Aps., Fredriksberg, Denmark). Probes were installed in the spring of 2003 in the MES beech stand; one probe was installed in an augered hole in each of the three main soil horizons (A_h, E and B_{21t}), at depths of 5, 20 and 50 cm, respectively. The soil solutions were obtained by connecting evacuated bottles (–50 kPa) to the porous probes. Sampling was made at different periods during the years 2003 and 2004. All materials for solution sampling were preconditioned with nanopure water before use.

Soil physical and chemical analysis

Soil samples were air-dried, gently crushed in a porcelain mortar and sieved to a particle size of < 2 mm. Particle-size distribution was determined by the pipette method after H₂O₂ pre-treatment and dispersion with Na-citrate. Common methods were used for the determination of soil pH (stiff paste soil-H₂O), exchangeable acidity and exchangeable aluminium (1 M KCl extraction; derivative titration curve for H⁺ and Al³⁺), exchangeable cations (1 M CH₃COONH₄ pH 7 extraction; ICP-OES determination of Ca, Mg, K and Sr concentrations),

carbon and carbonates (dry combustion; Ströhlein dosimeter) and nitrogen (semimicro Kjeldahl method). The soil organic matter content was assumed to be twice the amount of total carbon. In the organic-rich soil samples (A_h and E horizons), organically bound Ca and Sr concentrations were determined by ICP-OES after calcination at 450°C and dissolution of the ash with 0.1 M HCl. In both cases, amounts of exchangeable Ca and Sr were subtracted from the total amounts in these extracts.

Iron and aluminium were extracted with NH_4 -oxalate and Na-dithionite at 60°C ('free' Fe_{do} and Al_{do} ; Duchaufour & Souchier, 1966) and acid NH_4 -oxalate ('amorphous' Fe_{ox} and Al_{ox} ; Schwertmann, 1964); Fe and Al were determined by ICP-OES.

Total chemical analysis was made by fusion of 100 mg finely ground soil or clay, silt and sand fractions, at 700°C in Pt-Au crucibles (Claisse-Fluxy, Sainte-Foy, Canada) with Li-metaborate. Fused samples were dissolved in a 5% (by volume) HNO_3 solution and major elements were determined by ICP-OES. Sr, Zr, and Rb contents were determined by standard X-ray fluorescence spectrometry techniques on pressed powder pellets (~10 g of sample). Analyses were carried out on an ARL9400XP instrument (Thermo Electron Corporation, Waltham, USA), following the procedure described by Bologne & Duchesne (1991).

For the Sr isotopic analyses, bulk soil samples and clay- and silt-size separates were totally digested (~100 mg) in sealed Teflon vessels using a $HF-HNO_3$ (10:1) acid mixture. One sample that contains $CaCO_3$ (MES C_k horizon) was leached with 2.5 M HCl to dissolve its calcareous component selectively. The carbonated fraction of the C_k horizon of the loessic parent material was leached using suprapure 0.5 M CH_3COOH (only a partial dissolution was carried as a precaution against a possible acid attack of the silicate residue). Analyses of the clay and silt fractions of the C_k horizon were made on the silicate residue obtained by progressive decarbonation at $pH \geq 5$, with 0.1 M HCl.

Particle-size fractionation for XRD, total chemical analysis and Sr isotope analysis

The separation of clay (< 2 μm), fine silt (2–20 μm), coarse silt (20–50 μm) and sand (50–2000 μm) fractions was made using wet sieving (size range > 50 μm) or sedimentation (< 50 μm) after H_2O_2 pre-treatment and dispersion with Na citrate solution (final concentration of 0.8 g litre⁻¹) or, for the samples used for isotopic measurements, with a weakly acidic cation exchanger.

Mineralogical determinations

The mineralogical composition of clay- and silt-size separates was determined by XRD analyses on powder (silt fraction: 2–50 μm) or air-dried oriented samples on glass slides (clay fraction: < 2 μm); the diffraction was performed using a Bruker

GADDS diffractometer with Cu K_α radiation. The vermiculite content of the bulk soil was determined using the cation exchange capacity method of Coffman & Fanning (1974).

Quantitative mineralogical reconstitution and isotitane assessment method

The quantitative mineralogical reconstitution of the main soil minerals is based on the total chemical analysis of the bulk soil (< 2 mm), the clay (< 2 μm), the silt (2–50 μm) and the sand (50–2000 μm) fractions. Each mineral was reconstituted in proportion to a particular chemical element that is exclusive to it (e.g. Na for albite, Ca for anorthite, etc.) and on the basis of its theoretical formula (Lelong & Souchier, 1970). The relative amounts of the two K-bearing minerals (i.e. K-feldspar and muscovite) and the two Mg-bearing minerals (chlorite and green hornblende) were determined on both the silt (2–50 μm) and the sand (50–2000 μm) fractions of each soil horizon using the selective dissolution procedure of Kiely & Jackson (1965). The FeO/MgO molar ratio of the chloritic mineral was estimated on the basis of hot 1 M HCl extracts of the clay (< 2 μm) and silt (2–50 μm) fractions. More details on the analytical procedures are available in Sohet *et al.* (1988).

Assessment of quantitative mineralogical variations in soil profiles was made on an isotitane basis. The isotitane method allows determination of the absolute variations of a soil element or mineral relative to total TiO_2 content. A titanium-containing mineral such as rutile is a stable and resistant component in the NW Europe loess deposit. In addition, the distribution with depth of TiO_2 is similar to quartz or Nb, two other resistant constituents that justify its use in these profiles as a conservative element.

Soil extracts and soil solution for isotopic determinations

The *labile soil fraction* is defined as the sum of cations present in the soil solution and of 'exchangeable' cations adsorbed on mineral and organic soil colloids. This cation pool was extracted with suprapure CH_3COONH_4 (10 g soil with 50 ml 1 M CH_3COONH_4 at pH 7). The CH_3COONH_4 extracts were dried on a hot plate, and ashed in covered zirconium crucibles (16 hours at 450°C) to eliminate ammonium acetate. Ashes were dissolved with 1 ml suprapure HCl, heated on a hot plate for 10 minutes, avoiding boiling, and brought to a final volume of 50 ml; Ca and Sr concentrations were determined by ICP-OES.

'Acid extractable' fraction: the aim is to simulate natural release by weathering by dissolving selectively the more weatherable minerals (Miller *et al.*, 1993; Bullen & Bailey, 2005). Prior to the acid treatment, exchangeable cations were leached three times with suprapure 1 M CH_3COONH_4 solution and the residue was rinsed three times with nanopure water. Four successive acid extracts were obtained from the residue by shaking 5 g of soil with 50 ml suprapure 0.1 M HCl for

2 hours, centrifuging at 10000 g for 5 minutes and filtering to 0.45 μm (cellulose nitrate filters rinsed with acid). Ca, Mg, K, Na, Al, Fe and Sr were determined by ICP-OES in the acid extract. Surface horizons containing organic matter were at first treated with suprapure H_2O_2 30% at 90°C and afterwards leached with suprapure 1 M $\text{CH}_3\text{COONH}_4$ to eliminate exchangeable and organically bound cations. Sr procedural blanks were less than 3‰ of the sample concentrations for all the HCl extracts, and less than 5‰ of the sample concentrations for $\text{CH}_3\text{COONH}_4$ extracts, except for some E horizons (< 1%). Soil solutions collected on the field were stored at 4°C and analysed for Ca, Sr and Ba by ICP-OES.

Sr isotope analysis

Chemical separation of Sr was carried out by cation exchange chromatography. Sr isotopic compositions were measured on a VG Sector 54 multicollector thermal ionisation mass spectrometer (GV Instruments, Manchester, UK). The measured $^{87}\text{Sr}/^{86}\text{Sr}$ ratios were normalized to $^{86}\text{Sr}/^{88}\text{Sr} = 0.1194$. Measurements of the NBS-987 Sr standard yielded an average $^{87}\text{Sr}/^{86}\text{Sr}$ value of 0.710272 ± 0.000007 (2σ , $n = 18$). Additional details of the analytical procedure can be found in Ashwal *et al.* (2002).

The proportion of Sr in a mixture derived from two sources is calculated using a two-component (1 and 2) mixing equation (Capo *et al.*, 1998; Drouet *et al.*, 2005a):

$$X(\text{Sr})_1 = \frac{(^{87}\text{Sr}/^{86}\text{Sr})_{\text{Mix}} - (^{87}\text{Sr}/^{86}\text{Sr})_2}{(^{87}\text{Sr}/^{86}\text{Sr})_1 - (^{87}\text{Sr}/^{86}\text{Sr})_2} \quad (1)$$

where $X(\text{Sr})_1$ represents the mass fraction of Sr derived from source #1. Subscripts 1 and 2 refer to the two sources. The *Mix* subscript indicates the mixture component.

The relative contribution of Ca from two sources to a mixing component is given by a two-component mixing equation (Capo *et al.*, 1998):

$$X(\text{Ca})_1 = \frac{\left[(^{87}\text{Sr}/^{86}\text{Sr})_{\text{Mix}} - (^{87}\text{Sr}/^{86}\text{Sr})_2 \right] (\text{Sr}/\text{Ca})_2}{\left[(^{87}\text{Sr}/^{86}\text{Sr})_{\text{Mix}} - (^{87}\text{Sr}/^{86}\text{Sr})_2 \right] (\text{Sr}/\text{Ca})_2 + \left[(^{87}\text{Sr}/^{86}\text{Sr})_1 - (^{87}\text{Sr}/^{86}\text{Sr})_{\text{Mix}} \right] (\text{Sr}/\text{Ca})_1} \quad (2)$$

where $X(\text{Ca})_1$ represents the mass fraction of Ca derived from the atmospheric source.

Results and discussion

Soil physico-chemical properties and mineralogical composition

The analytical characterization of the soil profiles of the four forest sites studied is given in Table 1. The calcareous unweathered loess is frequently preserved in the lower part of the loess deposit, but only at a depth generally greater than 250 cm. Its

thickness is highly variable: from some decimetres (PIG and TUM sites) to several metres thick (MES and REL II sites). The unweathered loess contains 13% CaCO_3 (C_k horizon). The silicate fraction of unweathered loess contains more than 75% silt-size particles (2–50 μm), less than 10% sand (50–2000 μm) and around 14% clay (< 2 μm). The silt fraction is dominated by coarse silt (20–50 μm) and the sand fraction is exclusively composed of fine sand (< 100 μm). The similar particle-size distribution curves for samples taken at different depths in the six upper metres of the loess mantle in the MES site indicate that the niveo-aeolian deposit is remarkably homogeneous (Figure 1). The profile of the clay fraction shows a downward translocation of clay (illuviation process). The clay content is around 15% in the C horizon, 10% in the upper eluvial E horizon and 20% in the illuvial and clay-enriched B_{21t} horizon, which displays oriented clay coatings. The clay illuviation ratio (% clay B_{21t} /% clay E) in the profiles studied, ranges between 1.70 and 2.08. The presence of a clay-enriched horizon in the soil profile creates textural and structural variations and leads also to clear discontinuities for several chemical and mineralogical parameters. The vertical distribution of free-iron (Fe_{do}) fits well with the clay illuviation pattern, with a B_t/E free-iron ratio from 1.3 to 2.0. In contrast, the amounts of amorphous iron (Fe_{ox}) decrease with depth, in agreement with a decreasing weathering intensity (Table 1).

As determined by the mineralogical reconstitution, quartz (~55%) is the main mineral in the parent material. Other minerals present are muscovite (~20%), K-feldspar (~6%), Ca-plagioclase (3%) and Na-plagioclase (~15%), trioctahedral chlorite (~10%, including the < 2 μm soil fraction), kaolinite (~5%) and 2:1 micaceous clay minerals (~6%); expansible clay minerals (vermiculites and smectites) are also present in the clay fraction.

The complete dissolution of CaCO_3 in the calcareous loess and the subsequent desaturation of the exchange complex lower the pH- H_2O to ~5.0 in the B_{22t} and B_{31t} horizons (> 175 cm depth) and to 4.5 or less in the overlying B_{21t} and E horizons. The effective base cation saturation is around 90% in the B_{31t} horizons and decreases on average to 37% in the clay-enriched B_{21t} horizon and to 16% in the E horizon. These correspond to aluminium saturation increases from B_{31t} (~10%) to overlying horizons (> 50%). Humic layers are particularly acid (mean pH- H_2O = 3.7; mean exchangeable acidity = 5.1 $\text{cmol}_c \text{kg}^{-1}$) and have large organic matter contents (~12%). C/N ratios range from 14.7 to 21.3.

Quantitative mineralogical reconstitution and mineral losses by the isotitane assessment method

The total chemical composition of the bulk soil, the clay and the silt fractions used for the quantitative mineralogical reconstitutions of the soil profile of the MES site are given in Tables 2–5. The mineralogical compositions of the bulk soil, silt and clay fractions, expressed on an isotitane basis, are given in Table 6. TiO_2 -normalized losses or gains of minerals, expressed in per

cent of the initial reserve of the reference C_k horizon, are shown in Figure 2 for both MES and TUM sites.

The quartz contents of the bulk soil and the silt fraction clearly increase from the unweathered loess (C_k horizon) to the upper A_h horizon (from 55% to 71% for the bulk soil), whilst amounts of potentially more weatherable minerals decrease to varying degrees.

Of the primary silicate minerals present in the loess parent material (K-feldspar, plagioclase, trioctahedral chlorite, muscovite and associated 2:1 clay-minerals), two are readily weatherable in the local soil conditions: plagioclase and chlorite. Both are well known as weakly resistant minerals in an acid soil environment (Olson *et al.*, 2000), while muscovite and K-feldspar are considered to be more resistant. Our results indicate, from the bottom to the top of the soil profiles, a strong decrease of plagioclase (present in the silt and sand fractions) and of trioctahedral chlorite (present in sand, silt and clay fractions), in contrast to K-feldspar, which is comparatively less weathered. Calculated for the bulk soil in the MES site, TiO_2 -normalized losses of Ca-plagioclase are around 40% in the B_{31t} horizon, i.e. the lower part of the illuvial soil compartment, at around 2 m depth, at a short distance (~ 50 cm) from the decarbonation front (Figure 2a). In the TUM site, losses are $\sim 30\%$ at nearly the same distance from the C_k horizon (Figure 2b). This suggests that plagioclase weathering occurs rapidly after the decarbonation of the parent material. It also confirms the great weatherability of this mineral even in moderately acid conditions (pH- $H_2O \sim 5$). Half or more of the Ca-plagioclase content is lost in the overlying and more strongly acid (pH- $H_2O \sim 4.0$ or less) B_{21t} , E and A_h horizons, i.e. roughly the upper metre of the MES and TUM soil profiles. By contrast, the losses of K-feldspar in the same horizons are not greater than 25% and mainly around 10% or less at greater depths.

The weathering pattern of muscovite, which is frequently referred as a resistant mineral, is more surprising: losses of muscovite calculated for the bulk soil are equal to or greater than 50% in the upper metre of the acid-leached soil of the MES site. Owing to the great resistance of this mineral to chemical weathering, the observed decrease can probably be explained by the fact that silt-size mica is broken down physically into clay particles ('physical' weathering), a process which has been described in similar loessic soils by Van Ranst *et al.* (1982) and Brahy *et al.* (2000). The content of trioctahedral chlorite is also reduced in the eluvial and the humic layers, but clearly more strongly than muscovite. Nearly 60% to 80% of the initial content of the trioctahedral chlorite is lost in the surface horizons of the TUM and MES sites, respectively. These severe losses can be attributed to: (i) strongly acid conditions and a chelating soil environment, which promote ferromagnesian chemical weathering; (ii) a downward translocation process of clay-size chlorites, giving rise to a relative accumulation in the eluviated horizons of the immobile and poorly weatherable minerals (e.g. quartz and K-feldspar), a distinctive feature of acid 'leached' soils developed on loess; and (iii)

physical breakdown of silt-size chlorite, as suggested by Van Ranst *et al.* (1982). Greater resistance of K-feldspar and similar depletion of ferromagnesian minerals were also shown in similar soil conditions by Brahy *et al.* (2000). Lastly, the vertical distribution pattern of clay minerals shows clearly that both illites and vermiculites are translocated from the eluvial to the illuvial soil compartment (Table 6). The large vermiculite/illite ratios in the B_{21t} and B_{31t} horizons suggest that vermiculites are more subject to the illuviation process than illites. Smectites, to which neither the mineralogical reconstitution method nor a specific quantitative determination method can be applied, are thought to migrate in a similar way to vermiculites.

Evolution of the bulk soil $^{87}Sr/^{86}Sr$ ratio in relation to the mineralogical composition

The soil $^{87}Sr/^{86}Sr$ ratio depends on the Rb/Sr ratio and on the age of the parent material, because ^{87}Sr is produced by the radioactive β^- decay of ^{87}Rb (half-life $\sim 48.8 \times 10^9$ years) whereas ^{86}Sr is non-radiogenic (Faure, 1986). The Sr isotopic composition of each mineral is different and the bulk soil $^{87}Sr/^{86}Sr$ ratio is the weighted average of all its constituent minerals. In the soils studied, rubidium was concentrated mainly in K-feldspar, white micas and illitic clay minerals that have an increasing Sr isotopic ratio with time, whereas the Rb-poor and Sr-rich plagioclase will maintain a low $^{87}Sr/^{86}Sr$ ratio. Chlorite has a crystal structure that does not readily accept the large Ca^{2+} and Sr^{2+} ions or monovalent alkali cations in the lattice (Bailey *et al.*, 1996; Clow *et al.*, 1997). Chlorite is therefore thought to have a minor influence on the Sr isotopic distribution with depth, in spite of a well-marked weathering pattern. In the clay fraction, the weathering of illitic minerals to vermiculite (or smectite) is known to occur by replacement of K (and hence, Rb) in the interlayer sites of the 2:1 layer with hydrated exchangeable cations (Schulze, 2002). In the same way as for chloritic minerals, these 'swelling' minerals are consequently believed to have no or only a minor influence on the Sr isotopic distribution in soil profiles.

Total Sr contents and bulk soil $^{87}Sr/^{86}Sr$ ratios of the main horizons of the five soil profiles studied are given in Table 7. Table 8 shows the Ca and Sr contents of the Labile fraction and of the organic matter (A_h horizon) compared to those of the bulk soil. The Sr isotope compositions of the silt (2–50 μm) and the clay (< 2 μm) fractions were measured in the soil profile of the MES I site (Table 9). The distribution of the Sr isotopic ratio with depth is shown in Figures 3 and 4.

The $^{87}Sr/^{86}Sr$ ratio of the unweathered calcareous loess (C_k horizon) is on average 0.7169 ± 0.0015 (mean \pm SD, $n = 4$). The $^{87}Sr/^{86}Sr$ ratios of the calcareous fraction (0.5 M CH_3COONH_4 leachate) and of the silicate residue (HF digested after HCl leaching) were measured in the MES site and are 0.708255 and 0.725714, respectively. The five soil profiles show

Table 1 Soil physical and chemical properties of the four forest sites studied

Horizon	Sampling depth/cm	Particle size distribution				O.M./%	C/N	CaCO ₃ /%
		2000–50 μm	50–20 μm	20–2 μm	<2 μm			
		/% mineral soil fraction						
Mésanges site (MES), Dystric podzoluvisol								
A _h	0–5	n.d.	n.d.	n.d.	n.d.	21.3	18.3	0.0
E	5–25	6.0	57.9	26.0	10.1	2.2	14.7	0.0
B _{1t}	25–35	8.8	52.4	22.7	16.1	1.8	n.d.	0.0
B _{21t}	55–75	6.1	53.0	21.8	19.1	0.2	n.d.	0.0
B _{22t}	80–90	4.9	57.4	18.9	18.8	0.1	n.d.	0.0
B _{31t}	175–200	8.2	53.5	21.8	16.5	n.d.	n.d.	0.0
B _{32t}	210–220	4.1	53.5	25.3	17.1	n.d.	n.d.	0.0
B _{33t}	220–230	4.7	53.8	25.2	16.4	n.d.	n.d.	0.0
C	230–240	7.0	57.3	20.7	15.0	n.d.	n.d.	0.0
C _{k1}	245–250	n.d.	n.d.	n.d.	n.d.	n.d.	n.d.	9.8
C _{k2}	255–290	6.8	49.8	17.1	14.2	n.d.	n.d.	13.7
Relais des Dames II site (REL II), Dystric podzoluvisol								
A _h	0–5	n.d.	n.d.	n.d.	n.d.	28.3	17.6	0.0
E	5–25	5.6	47.5	36.0	10.8	1.07	6.6	0.0
B _{21t}	55–75	6.1	52.0	21.8	20.1	n.d.	n.d.	0.0
B _{31t}	175–200	5.5	47.2	29.7	17.7	n.d.	n.d.	0.0
C _k	260–300	n.d.	n.d.	n.d.	n.d.	n.d.	n.d.	15.8
Tir aux Pigeons site (PIG), Dystric podzoluvisol								
A _h	0–5	n.d.	n.d.	n.d.	n.d.	17.6	14.7	0.0
E	5–25	7.1	59.4	23.7	9.8	n.d.	n.d.	0.0
B _{21t}	55–75	6.7	58.1	18.4	16.8	n.d.	n.d.	0.0
B _{31t}	175–200	12.1	58.3	15.5	14.1	n.d.	n.d.	0.0
C _k	360–380	n.d.	n.d.	n.d.	n.d.	n.d.	n.d.	3.2
Tumuli site (TUM), Dystric podzoluvisol								
A _h	0–5	n.d.	n.d.	n.d.	n.d.	27.3	21.3	0.0
E	5–25	10.7	49.0	28.0	12.4	0.5	22.9	0.0
B _{21t}	55–75	5.2	47.4	26.3	21.1	n.d.	n.d.	0.0
B _{31t}	175–200	4.9	47.4	30.4	17.3	n.d.	n.d.	0.0
C _k	360–380	8.8	51.5	27.9	11.8	n.d.	n.d.	10.5
2C _k	400–425	19.8	n.d.	n.d.	n.d.	n.d.	n.d.	8.3
Mean \pm S.D.^b								
A _h	0–5	n.d.	n.d.	n.d.	n.d.	23.5 \pm 5.1	17.8 \pm 2.7	
E	5–25	7.1 \pm 2.3	55.1 \pm 6.0	27.5 \pm 5.4	10.3 \pm 1.2	1.3 \pm 0.9	13.5 \pm 8.2	
B _{21t}	55–75	6.6 \pm 0.6	53.6 \pm 4.4	21.7 \pm 3.2	18.1 \pm 1.9	n.d.	n.d.	
B _{31t}	175–200	6.6 \pm 3.3	52.1 \pm 5.4	24.8 \pm 7.1	16.5 \pm 1.6	n.d.	n.d.	

^an.d. = not determined.^bS.D. = standard deviation.

Table 1 Continued

Horizon	pH-H ₂ O	Exchangeable ^a acidity /cmol _c kg ⁻¹	Exchangeable cations ^b			Exchangeable ^a Al ³⁺ /cmol _c kg ⁻¹	Effective CEC /cmol _c kg ⁻¹	Effective saturation rate/%	Calcium saturation rate/%	Aluminium iron ^c (Fe _{ox})/%	Amorphous aluminium ^c (Al _{ox})/%	Amorphous aluminium ^c (Al _{ox})/%	Free iron ^d (Fe _{do})/%
			Ca ²⁺	Mg ²⁺	K ⁺								
Mésanges site (MES), Dystric podzoluvisol													
A _h	3.7	3.28	1.56	0.46	0.39	1.35	5.69	42.4	27.4	23.7	0.35	0.12	0.63
E	4.0	2.59	0.32	0.10	0.12	2.52	3.13	17.3	10.2	80.5	0.44	0.16	0.55
B _{1t}	4.1	2.98	0.20	0.10	0.15	2.98	3.43	13.1	5.8	86.9	0.36	0.20	0.77
B _{21t}	4.2	3.05	1.09	0.20	0.20	2.48	4.54	32.8	24.0	54.6	0.22	0.12	0.81
B _{22t}	4.4	2.26	1.97	0.93	0.21	2.26	5.37	57.9	36.7	42.1	0.20	0.14	0.32
B _{31t}	4.9	1.29	5.09	2.41	0.27	1.29	9.06	85.8	56.2	14.2	0.08	0.07	n.d.
B _{32t}	5.0	0.21	8.40	3.42	0.19	0.21	12.22	98.3	68.7	1.7	n.d.	n.d.	n.d.
B _{33t}	5.1	0.29	8.15	3.48	0.20	0.29	12.12	97.6	67.2	2.4	n.d.	n.d.	n.d.
C	5.3	0.00	10.32	2.80	0.18	0.00	13.30	100.0	77.6	0.0	n.d.	n.d.	n.d.
C _{k1}	6.7	n.d. ^e	n.d.	n.d.	n.d.	n.d.	n.d.	n.d.	n.d.	n.d.	n.d.	n.d.	n.d.
C _{k2}	7.7	n.d.	n.d.	n.d.	n.d.	n.d.	n.d.	n.d.	n.d.	n.d.	0.05	0.14	n.d.
Relais des Dames II site (REL II), Dystric podzoluvisol													
A _h	3.7	5.87	0.44	0.67	0.62	4.60	7.60	22.8	5.8	60.5			
E	4.2	2.71	0.13	0.06	0.08	2.53	2.98	9.1	4.4	84.9			
B _{21t}	4.4	5.11	1.18	0.52	0.21	4.84	7.02	27.2	16.8	68.9			
B _{31t}	5.0	0.59	5.35	2.25	0.19	0.59	8.38	93.0	63.8	7.0			
C _k	7.9	n.d.	n.d.	n.d.	n.d.	n.d.	n.d.	n.d.	n.d.	n.d.			
Tir aux Pigeons site (PIG), Dystric podzoluvisol													
A _h	3.8	5.24	1.38	0.68	0.39	3.76	7.69	31.9	17.9	48.9			
E	4.3	2.26	0.20	0.11	0.12	2.18	2.69	16.0	7.4	81.0			
B _{21t}	4.5	3.19	1.53	1.38	0.24	2.94	6.34	49.7	24.1	46.4			
B _{31t}	5.0	0.94	6.35	3.01	0.19	0.75	10.49	91.0	60.5	7.1			
C _k	7.9	n.d.	n.d.	n.d.	n.d.	n.d.	n.d.	n.d.	n.d.	n.d.			
Tumuli site (TUM), Dystric podzoluvisol													
A _h	3.7	5.92	0.34	0.43	0.37	4.01	7.06	16.1	4.8	56.8			
E	4.3	1.67	0.25	0.09	0.10	1.57	2.11	20.9	11.8	74.4			
B _{21t}	4.5	5.80	1.88	1.20	0.29	4.02	9.17	36.8	20.5	43.8			
B _{31t}	5.0	0.68	5.00	2.07	0.21	0.68	7.96	91.5	62.8	8.5			
C _k	7.9	n.d.	n.d.	n.d.	n.d.	n.d.	n.d.	n.d.	n.d.	n.d.			
2C _k	7.9	n.d.	n.d.	n.d.	n.d.	n.d.	n.d.	n.d.	n.d.	n.d.			
Mean ± S.D.^f													
A _h	3.7 ± 0.1	5.1 ± 1.2	0.9 ± 0.6	0.6 ± 0.1	0.44 ± 0.12	3.4 ± 1.4	7.0 ± 0.9	28.3 ± 11.4	14.0 ± 10.8	47.5 ± 16.6			
E	4.2 ± 0.1	2.3 ± 0.5	0.2 ± 0.1	0.09 ± 0.02	0.11 ± 0.02	2.2 ± 0.5	2.7 ± 0.5	15.8 ± 4.9	8.5 ± 3.3	80.2 ± 4.3			
B _{21t}	4.4 ± 0.1	4.3 ± 1.4	1.4 ± 0.4	0.8 ± 0.6	0.24 ± 0.04	3.6 ± 1.1	6.8 ± 1.9	36.6 ± 9.6	21.4 ± 3.5	53.4 ± 11.3			
B _{31t}	5.0 ± 0.1	0.9 ± 0.3	5.4 ± 0.6	2.4 ± 0.4	0.22 ± 0.04	0.8 ± 0.3	9.0 ± 1.1	90.3 ± 3.1	60.8 ± 3.4	9.2 ± 3.4			

^aExtraction with 1 M KCl.^bExtraction with 1 M CH₃COONH₄ pH 7.^cExtraction with acid ammonium oxalate pH 3.4.^dExtracton with acid ammonium oxalate and Na dithionite at 60°C.^en.d., not determined.^fS.D., standard deviation.

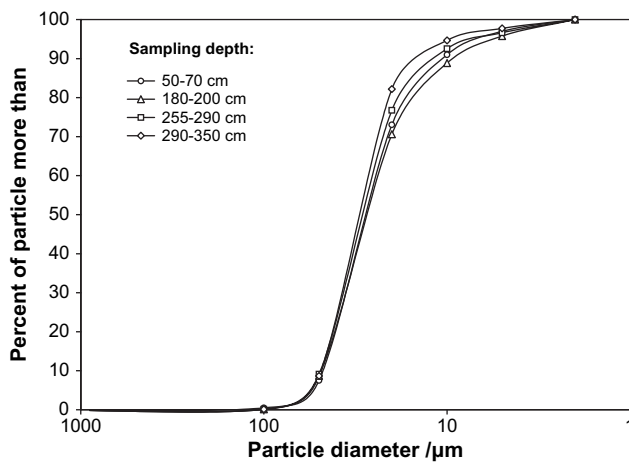


Figure 1 Particle-size distribution curves for different sampling depths in the 3.5 upper metres of the loessic deposit in the MES site.

a similar distribution pattern of their $^{87}\text{Sr}/^{86}\text{Sr}$ ratio with depth (Figure 3a). In the B_{31t} horizons (175–200 cm depth), the Sr isotope ratio is on average 0.7279 ± 0.0015 , slightly larger than the Sr isotope composition of the silicate residue of the carbonated loess measured in the MES I soil profile ($^{87}\text{Sr}/^{86}\text{Sr} = 0.725714$). This slight increase of the isotope ratio can be attributed to a larger proportion of radiogenic (K- and Rb-rich) mineral due to the weathering of the most weatherable mineral, i.e. Ca-plagioclase, which is promoted by a strong decrease of the soil pH (pH-H₂O in the C_k and the B_{31t} horizons are ~ 7.5 and ~ 5.0 , respectively).

In the overlying clay-enriched B_{21t} horizon (55–75 cm depth), the increase of the Sr isotopic ratio (on average, $^{87}\text{Sr}/^{86}\text{Sr} = 0.73234 \pm 0.00053$, $n = 5$) is also consistent with a more severe weathering environment due to increasing acidity (pH < 4.5). The isotitane assessment method (Table 6, Figure 4) has shown that around 40 and 50% of the initial content of the Ca-plagioclase in the C_k horizon was lost in the B_{31t} and B_{21t} horizons, respectively. Hence, the evolution of the $^{87}\text{Sr}/^{86}\text{Sr}$

Table 2 Total chemical compositions of the bulk soil (fine earth < 2 mm) of five soil profiles representative of the sites studied (MES I and MES II are two different soil profiles sampled in the main MES site). Results are expressed in wt. %

Site	Horizon	Sampling depth/cm	SiO ₂	Al ₂ O ₃	CaO	K ₂ O	MgO	Na ₂ O	Fe ₂ O ₃	MnO	TiO ₂	L.I.	Sum
			/ %										
MES I	A _h	0–5	72.13	5.86	0.35	1.63	0.22	0.84	1.63	0.02	0.64	18.3	101.6
	E	5–25	86.89	6.17	0.36	1.54	0.31	0.85	1.88	0.06	0.78	4.00	102.8
	B _{21t}	55–75	82.96	9.35	0.31	1.91	0.89	0.98	4.24	0.09	0.78	2.28	103.8
	B _{31t}	175–200	77.80	9.38	0.56	1.98	0.82	1.12	3.62	0.07	0.79	3.81	100.0
	C _k	300–320	67.26	7.63	7.42	1.66	1.37	0.91	3.02	0.06	0.65	8.10	98.1
MES II	A _h	0–5	67.26	5.86	0.28	1.48	0.27	0.81	1.72	0.02	0.61	19.36	98.0
	E	5–25	84.70	6.91	0.30	1.88	0.28	1.02	1.73	0.06	0.73	4.00	101.6
	B _{21t}	55–75	78.38	9.62	0.27	2.21	0.68	0.96	3.62	0.08	0.70	4.08	100.6
	B _{31t}	175–200	80.43	8.83	0.47	1.93	0.81	0.94	3.68	0.07	0.69	4.58	102.4
	C _k	300–320	75.19	7.19	5.34	1.66	0.97	1.10	2.98	0.07	0.61	7.06	102.2
REL II	A _h	0–5	67.88	5.35	0.29	1.44	0.22	0.79	1.50	0.03	0.59	23.14	101.2
	E	5–25	84.33	6.39	0.30	1.75	0.24	0.97	1.55	0.04	0.72	3.71	100.0
	B _{21t}	55–75	79.77	9.13	0.30	2.08	0.66	0.93	3.39	0.06	0.70	4.40	101.4
	B _{31t}	175–200	82.79	9.94	0.50	2.24	0.81	1.12	3.53	0.09	0.68	4.19	105.9
	C _k	450–470	73.76	6.44	6.72	1.47	1.24	1.02	2.60	0.05	0.58	8.70	102.6
PIG	A _h	0–5	65.86	5.79	0.33	1.52	0.29	0.84	2.07	0.03	0.57	23.33	100.6
	E	5–25	84.27	6.56	0.29	1.73	0.29	1.01	1.72	0.03	0.70	4.17	100.8
	B _{21t}	55–75	79.65	8.67	0.29	1.97	0.61	0.96	3.14	0.07	0.67	4.12	100.2
	B _{31t}	175–200	80.43	8.45	0.46	2.12	0.68	1.31	3.10	0.06	0.67	3.49	100.8
	C _k	360–380	70.92	7.46	4.47	1.61	0.77	0.8	3.13	0.07	0.67	6.76	96.7
TUM	A _h	0–5	58.75	4.78	0.22	1.27	0.16	0.70	1.32	0.02	0.51	31.97	99.7
	E	5–25	85.97	6.62	0.31	1.91	0.26	1.06	1.78	0.07	0.73	3.18	101.9
	B _{21t}	55–75	78.17	9.59	0.31	2.28	0.70	0.97	3.62	0.12	0.70	4.82	101.3
	B _{31t}	175–200	78.44	9.78	0.50	2.32	0.81	1.18	3.61	0.08	0.69	4.15	101.6
	C _k	360–380	69.19	7.46	7.44	1.70	1.23	1.04	3.07	0.07	0.60	8.00	99.8
Mean ± S.D.													
(n = 5)	A _h	0–5	66.4 ± 4.9	5.5 ± 0.5	0.29 ± 0.05	1.47 ± 0.13	0.23 ± 0.05	0.80 ± 0.06	1.65 ± 0.28	0.02 ± 0.01	0.58 ± 0.05	23.22 ± 5.38	–
	E	5–25	85.2 ± 1.2	6.5 ± 0.3	0.31 ± 0.03	1.76 ± 0.15	0.28 ± 0.03	0.98 ± 0.08	1.73 ± 0.12	0.05 ± 0.02	0.73 ± 0.03	3.81 ± 0.39	–
	B _{21t}	55–75	79.8 ± 1.9	9.3 ± 0.4	0.30 ± 0.02	2.09 ± 0.16	0.71 ± 0.11	0.96 ± 0.02	3.60 ± 0.41	0.08 ± 0.02	0.71 ± 0.04	3.94 ± 0.97	–
	B _{31t}	175–200	80.0 ± 2.0	9.3 ± 0.6	0.50 ± 0.04	2.12 ± 0.17	0.79 ± 0.06	1.13 ± 0.13	3.51 ± 0.23	0.07 ± 0.01	0.70 ± 0.05	4.04 ± 0.41	–
	C _k	>300	71.3 ± 3.2	7.2 ± 0.5	6.28 ± 1.32	1.62 ± 0.09	1.12 ± 0.24	0.97 ± 0.12	2.96 ± 0.21	0.06 ± 0.01	0.62 ± 0.04	7.72 ± 0.80	–

S.D. for standard deviation.

L.I. for the loss-on-ignition at 1000°C.

Table 3 Molar ratios of the bulk soil total chemical composition of five profiles representative of the studied sites

Site	Horizon	SiO ₂ /CaO	SiO ₂ /Na ₂ O	SiO ₂ /K ₂ O	SiO ₂ /MgO	SiO ₂ /Al ₂ O ₃	SiO ₂ /Fe ₂ O ₃
MES I	A _h	192.4	88.6	69.4	220.1	20.9	117.7
	E	225.4	105.5	88.5	188.2	23.9	122.9
	B _{21t}	251.2	87.4	68.1	62.6	15.1	52.0
	B _{31t}	129.7	71.7	61.6	63.7	14.1	57.1
	C _k	8.5	76.3	63.5	33.0	15.0	59.2
MES II	A _h	225.5	86.2	71.7	168.1	19.6	104.5
	E	263.6	85.7	70.7	203.1	20.8	130.2
	B _{21t}	271.1	84.3	55.6	77.4	13.8	57.6
	B _{31t}	159.8	88.3	65.4	66.7	15.5	58.1
	C _k	13.1	70.6	71.0	52.0	17.7	67.1
REL II	A _h	218.6	88.7	73.9	207.1	21.5	120.3
	E	262.5	89.7	75.6	235.9	22.4	144.7
	B _{21t}	248.3	88.5	60.2	81.1	14.8	62.6
	B _{31t}	154.6	76.3	58.0	68.6	14.1	62.4
	C _k	10.2	74.6	78.7	39.9	19.4	75.4
PIG	A _h	186.4	80.9	68.0	152.5	19.3	84.6
	E	271.3	86.1	76.4	195.1	21.8	130.3
	B _{21t}	256.5	85.6	63.4	87.7	15.6	67.4
	B _{31t}	163.3	63.4	59.5	79.4	16.2	69.0
	C _k	14.8	91.5	69.1	61.8	16.1	60.2
TUM	A _h	249.3	86.6	72.6	246.5	20.9	118.3
	E	258.9	83.7	70.6	222.0	22.0	128.4
	B _{21t}	235.5	83.2	53.8	75.0	13.8	57.4
	B _{31t}	146.5	68.6	53.0	65.0	13.6	57.8
	C _k	8.7	68.7	63.8	37.8	15.7	59.9
Mean ± S.D.							
(n = 5)	A _h	214 ± 26	86.2 ± 3.2	71.1 ± 2.4	199 ± 38	20.4 ± 0.9	109.1 ± 15.1
	E	256 ± 18	90.2 ± 8.9	76.3 ± 7.3	209 ± 20	22.2 ± 1.1	131.3 ± 8.1
	B _{21t}	252 ± 13	85.8 ± 2.2	60.2 ± 5.8	77 ± 9	14.6 ± 0.8	59.4 ± 5.8
	B _{31t}	151 ± 13	73.7 ± 9.4	59.5 ± 4.6	69 ± 6	14.7 ± 1.1	60.9 ± 5.0
	C _k	11 ± 3	76.3 ± 9.0	69.2 ± 6.2	45 ± 12	16.8 ± 1.8	6.44 ± 6.9

S.D. for standard deviation.

isotope ratio reflects the weathering pattern of this Ca-bearing mineral and the increased proportion of resistant Rb-containing minerals like K-feldspar, as shown by the distributions with depth of the ⁸⁷Sr/⁸⁶Sr ratio, the SiO₂/CaO molar ratio and the ratio between K-feldspar and Ca-plagioclase, both in the bulk soil (Figure 3a,b,c) and the silt fraction (Figure 4a,c, Table 5). This clearly confirms that the evolution of the Sr isotope composition was mainly determined by the differential weatherability of strontium-bearing minerals, as previously noted by Åberg *et al.* (1989), Bain & Bacon (1994) and Bailey *et al.* (1996). More precisely, preferential weathering during soil forming processes of Ca- and Sr-rich minerals with a low ⁸⁷Sr/⁸⁶Sr ratio (i.e. Ca-plagioclase), compared with K- and Rb-rich minerals (mainly K-feldspar), explains most of the Sr isotopic pattern from unweathered loess to illuvial B_{31t} and B_{21t} horizons (Figure 4c). This suggests that the Ca-plagioclase, in spite of its small content in these acid, leached soils (< 3.5%), is of primary importance in determining the bulk soil Sr isotopic pattern.

Acidity still increases upwards in the soil profile and the most acid horizons are the eluvial E horizon (pH-H₂O~4.0) and the humic layer (pH-H₂O~3.7). One may therefore expect that the strengthening of weathering in this clay-depleted and organically enriched soil compartment will lead to a continuous increase of the Sr isotope ratio. Nevertheless, the Sr isotopic ratios of the E and B_{21t} horizons were very close (on average, 0.7321 ± 0.0001 versus 0.7323 ± 0.0005; n = 5, respectively) and clearly decrease (0.7301 ± 0.0025, n = 5) in the organic-rich humic layer (Figure 3). The decrease of the Sr isotopic value measured in the A_h organic horizon has been observed in other soils and has frequently been interpreted as an effect of the relatively unradiogenic Sr of litter returns and atmospheric deposition (Åberg *et al.*, 1989; Bain & Bacon, 1994; Bailey *et al.*, 1996; Poszwa *et al.*, 2004). Such a hypothesis is attractive, knowing that in the soil studied the humic layer contains around 20% of organic matter, mainly supplied by litterfall with a low Sr isotopic ratio (⁸⁷Sr/⁸⁶Sr ratio of beech leaves collected in the forest sites studied is, on average,

Table 4 Total chemical compositions of the clay (< 2 µm), the silt (2–50 µm) and the sand (50–2000 µm) fractions of the MES I soil profile. Results are expressed in wt.%

Sampling depth/cm	Horizon	SiO ₂	Al ₂ O ₃	CaO	K ₂ O	MgO	Na ₂ O	Fe ₂ O ₃	MnO	TiO ₂	L.I.	Sum
		/ %										
Clay fraction (<2 µm)												
0–5	A _h	57.21	15.67	0.42	2.02	1.21	0.16	8.60	0.03	0.94	12.10	98.36
5–25	E	55.05	18.56	0.74	2.31	1.49	0.23	7.50	0.11	1.04	14.10	101.12
55–75	B _{21t}	48.60	18.05	0.89	2.43	2.00	0.14	10.13	0.07	0.74	13.18	96.21
175–200	B _{31t}	49.17	23.48	0.19	2.56	2.37	0.18	13.16	0.11	0.90	13.90	106.02
300–320	C _{k1}	53.36	18.97	0.11	2.71	2.42	0.24	10.24	0.03	0.69	15.46	104.23
Silt fraction (2–50 µm)												
0–5	A _h	87.28	5.49	0.40	1.96	0.16	1.10	1.04	0.02	0.79	1.98	100.22
5–25	E	92.69	7.13	0.42	1.74	0.22	1.10	1.08	0.03	0.83	0.95	106.19
55–75	B _{21t}	88.43	6.28	0.48	1.87	0.42	0.95	1.71	0.03	0.73	1.32	102.21
175–200	B _{31t}	82.57	7.98	0.63	3.24	0.57	1.97	2.51	0.06	0.83	1.30	101.65
300–320	C _{k1}	82.78	7.55	0.79	3.16	0.58	2.09	2.75	0.05	0.63	1.93	102.31
Sand fraction (50–2000 µm)												
0–5	A _h	89.50	2.92	0.13	1.10	0.07	0.49	0.29	0.01	0.15	0.45	95.09
5–25	E	83.98	3.79	0.18	1.29	0.11	0.62	2.15	0.09	0.40	0.61	93.22
55–75	B _{21t}	87.95	3.67	0.11	1.37	0.10	0.62	0.57	0.02	0.21	0.44	95.06
175–200	B _{31t}	90.92	3.33	0.17	1.22	0.06	0.67	0.18	0.01	0.11	0.23	96.89
300–320	C _{k1}	72.13	5.86	0.35	1.63	0.22	0.84	1.63	0.02	0.64	21.30	104.62

L.I. for the loss-on-ignition at 1000°C.

0.711240 ± 0.00202, $n = 4$; Drouet *et al.*, 2005a). Moreover, the contribution of organic and exchangeable calcium to the total calcium pool was not negligible (~11%; Table 8). However, the influence of the organic and exchangeable Sr pools on the bulk soil isotopic ratio is most likely very small, as the exchangeable and the organically bound strontium represent

less than 2% of the total Sr content in the A_h horizon (Table 8), i.e. five times less than for calcium. This statement is reinforced by the fact that the silt fraction, which does not contain any biological or labile component, displays the same Sr isotopic distribution pattern as the bulk soil (Figures 4a and 5a).

Table 5 Molar ratios of the total chemical composition of the clay (< 2 µm), the silt (2–50 µm) and the sand (50–2000 µm) fractions of the MES I soil profile

Sampling depth/cm	Horizon	SiO ₂ /CaO	SiO ₂ /Na ₂ O	SiO ₂ /K ₂ O	SiO ₂ /MgO	SiO ₂ /Al ₂ O ₃	SiO ₂ /Fe ₂ O ₃
Clay fraction (<2 µm)							
0–5	A _h	137.8	354.8	28.3	47.3	3.7	6.7
5–25	E	74.5	236.7	23.9	37.0	3.0	7.3
55–75	B _{21t}	54.9	350.2	20.0	24.4	2.7	4.8
175–200	B _{31t}	258.8	273.2	19.2	20.7	2.1	3.7
300–320	C _{k1}	485.1	222.3	19.7	22.0	2.8	5.2
Silt fraction (2–50 µm)							
0–5	A _h	218.2	79.3	44.5	545.5	15.9	83.9
5–25	E	220.7	84.3	53.3	421.3	13.0	85.8
55–75	B _{21t}	185.7	93.3	47.3	210.6	14.1	51.9
175–200	B _{31t}	130.2	42.0	25.5	144.5	10.4	32.9
300–320	C _{k1}	104.4	39.7	26.2	143.8	11.0	30.1
Sand fraction (50–2000 µm)							
0–5	A _h	703.8	183.1	81.5	1343.7	30.7	312.7
5–25	E	466.9	134.7	65.3	775.1	22.1	39.0
55–75	B _{21t}	785.4	142.4	64.0	925.0	24.0	154.2
175–200	B _{31t}	550.0	134.7	74.8	1643.2	27.3	519.5
300–320	C _{k1}	206.1	85.9	44.3	327.9	12.3	44.3

Table 6 Quantitative mineralogical reconstitution of the MES I soil profile by an isotitane assessment method

Depth /cm	Horizon	Hornblende	K-feldspar	Muscovite	Illite	Na-plagioclase /wt.-%	Ca-plagioclase	Chlorite	Quartz	Vermiculite ^a
Bulk soil (<2 mm)										
0–5	A _h	0.3	6.9	9.5	2.9	9.0	1.8	3.5	71.0	0.8
10–15	E	0.3	6.4	8.3	3.3	8.5	1.8	3.3	68.8	0.5
55–75	B _{21t}	0.2	7.1	12.1	7.1	7.6	2.1	7.5	64.1	1.4
175–200	B _{31t}	0.2	7.5	19.8	5.7	15.5	2.8	9.9	51.9	1.3
300–320	C _k	0.3	6.4	20.5	5.7	16.3	3.5	9.0	54.9	0.7
Clay (2 µm)										
0–5	A _h	n.p. ^b	n.p.	n.p.	29.3	n.p.	n.p.	13.9	41.8	8.0
10–15	E	n.p.	n.p.	n.p.	33.1	n.p.	n.p.	12.5	34.8	5.1
55–75	B _{21t}	n.p.	n.p.	n.p.	37.0	n.p.	n.p.	21.4	30.3	8.8
175–200	B _{31t}	n.p.	n.p.	n.p.	33.5	n.p.	n.p.	25.9	16.8	7.3
300–320	C _k	n.p.	n.p.	n.p.	37.8	n.p.	n.p.	19.4	29.8	4.1
Silt (2–50 µm)										
0–5	A _h	0.3	6.6	7.5	n.p.	9.5	1.9	1.7	75.2	n.p.
10–15	E	0.3	6.2	5.2	n.p.	8.9	1.9	1.9	73.7	n.p.
55–75	B _{21t}	0.3	7.0	5.8	n.p.	8.0	2.3	3.3	73.9	n.p.
175–200	B _{31t}	0.2	7.5	16.7	n.p.	16.7	3.1	5.1	61.6	n.p.
300–320	C _k	0.2	6.5	17.3	n.p.	17.6	3.8	6.0	61.6	n.p.
Sand (50–2000 µm)										
0–5	A _h	0.4	10.4	3.5	n.p.	2.5	0.2	10.9	60.3	n.p.
10–15	E	0.4	9.5	9.4	n.p.	2.9	0.3	7.9	57.2	n.p.
55–75	B _{21t}	0.4	7.9	11.1	n.p.	2.5	0.1	15.2	49.8	n.p.
175–200	B _{31t}	0.4	7.1	17.2	n.p.	2.7	0.2	19.5	39.6	n.p.
300–320	C _k	0.6	4.5	15.7	n.p.	3.6	0.1	17.4	41.4	n.p.

^aDetermined by the method of Coffman & Fanning (1974) (see text).

^bn.p. = not present.

Our explanation is therefore that in loessial soils the main source that controls the bulk soil Sr isotopic ratio through the whole profile is weathering, rather than biotic processes. Mineralogical changes can be induced by downward transloca-

tion of minerals with high isotopic ratios (clay illuviation of illites) and by physical breakdown of muscovite and chemical weathering of K-feldspar in a more acidic soil environment (pH-H₂O < 4) (Olson *et al.*, 2000; Kohut & Warren, 2000). Increasing losses of

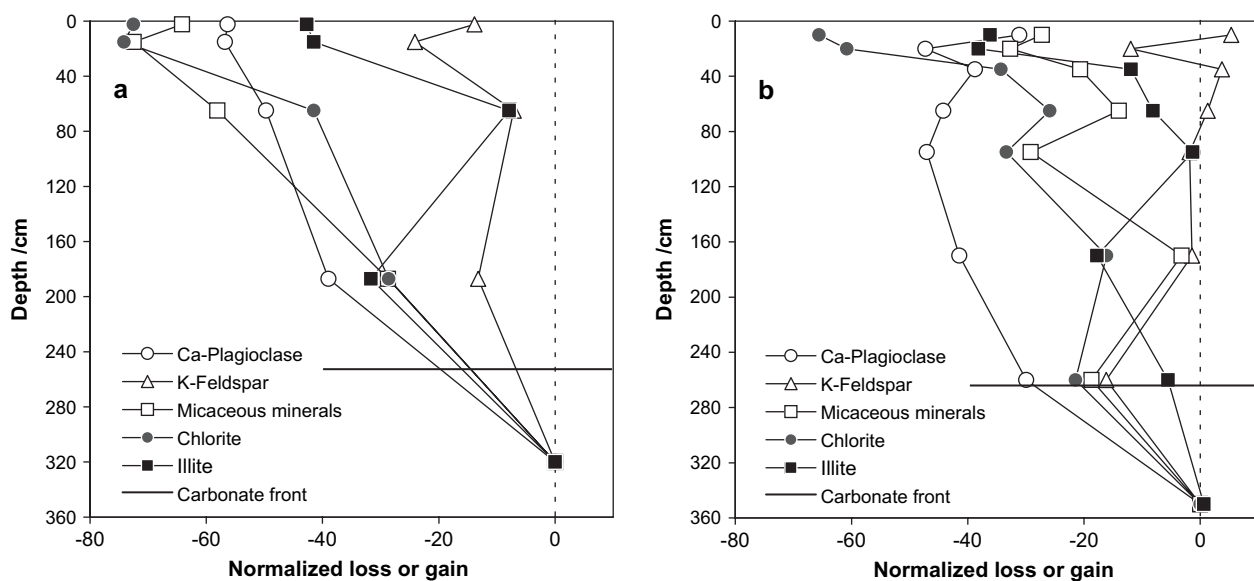


Figure 2 TiO₂-normalized losses or gains of minerals (% of the initial content of the C_k horizon) of (a) the MES I soil profile and (b) the TUM soil profile (redrawn from the data in El Bayad, 1996).

Table 7 $^{87}\text{Sr}/^{86}\text{Sr}$ ratios, Ca and Sr concentrations and Sr/Ca mass ratios of the bulk soil, the labile fraction and the HCl extracts in the MES I and MES II (after Drouet *et al.*, 2005a, with permission), TUM, PIG and REL II soil profiles. Rb concentrations are given for the bulk soil. $^{87}\text{Sr}/^{86}\text{Sr}$ ratios, Ca and Sr concentrations and Sr/Ca mass ratios of the soil solution are given for the MES site. Uncertainties on the isotopic data are reported as the 2-sigma error $\times 10^{-6}$

Location	Sampling depth /cm	Horizon	Bulk soil (sieved <2 mm)				0.1 M HCl leachate				
			$^{87}\text{Sr}/^{86}\text{Sr}$ $\pm 2\sigma \times 10^{-6}$	Sr /mg kg ⁻¹	Ca /mg kg ⁻¹	Rb /mg kg ⁻¹	Sr/Ca /g g ⁻¹	$^{87}\text{Sr}/^{86}\text{Sr}$ $\pm 2\sigma \times 10^{-6}$	Sr /mg kg ⁻¹	Ca /mg kg ⁻¹	Sr/Ca /g g ⁻¹
MES I	0–5	A _h	0.731066 ± 11	74.1	2500	67.8	0.0296	n.d.	n.d.	n.d.	n.d.
	10–25	E	0.732199 ± 14	83.5	3192	n.d.	0.0261	n.d.	0.14	12	0.0114
	55–75	B _{21t}	0.732698 ± 20	85.9	4429	n.d.	0.0194	n.d.	n.d.	n.d.	n.d.
	175–200	B _{31t}	0.727883 ± 16	92.8	3998	n.d.	0.0232	n.d.	0.73	159	0.0046
	300–320	C _k ^(b)	0.725714 ± 13	77.7	n.d.	69.5	n.d.	n.d.	n.d.	n.d.	n.d.
	300–320	Carbonates ^(a)	0.708255 ± 7	n.d. ^d	n.d.	n.d.	0.0022	n.d.	n.d.	n.d.	n.d.
	300–320	C _k	0.716592 ± 12	168.0	53031	60.0	0.0032	n.d.	n.d.	n.d.	n.d.
MES II	0–5	A _h	0.731109 ± 7	78.6	2035	73.1	0.0386	0.713643 ± 7	0.37	32	0.0117
	10–25	E	0.732115 ± 7	73.5	2161	61.0	0.0340	0.713114 ± 6	0.14	8	0.0179
	55–75	B _{21t}	0.732764 ± 10	75.9	1962	83.2	0.0387	0.712067 ± 7	0.39	15	0.0257
	175–200	B _{31t}	0.727066 ± 7	82.8	2929	83.0	0.0283	0.713571 ± 6	0.15	281	0.0041
TUM	0–5	A _h	0.725649 ± 6	88.3	1552	70.6	0.0569	n.d.	n.d.	n.d.	n.d.
	10–25	E	0.732008 ± 12	70.3	2205	60.7	0.0319	n.d.	0.12	8	0.0152
	55–75	B _{21t}	0.732556 ± 10	72.3	2195	77.9	0.0329	n.d.	0.32	25	0.0126
	175–200	B _{31t}	0.729223 ± 11	82.6	3592	80.3	0.0230	n.d.	1.64	488	0.0034
	360–380	C _k	0.717135 ± 10	155.1	n.d.	37.7	n.d.	n.d.	n.d.	n.d.	n.d.
REL II	0–5	A _h	0.731374 ± 15	79.1	2038	70.4	0.0388	n.d.	n.d.	n.d.	n.d.
	10–25	E	0.732282 ± 7	73.3	2178	60.1	0.0377	n.d.	0.15	13	0.0110
	55–75	B _{21t}	0.732199 ± 10	76.6	2131	79.5	0.0359	n.d.	0.42	14	0.0293
	175–200	B _{31t}	0.729445 ± 9	87.9	3557	84.3	0.0247	n.d.	1.74	439	0.0040
	260–300	C _k	0.714917 ± 10	168.2	n.d.	60.2	n.d.	n.d.	n.d.	n.d.	n.d.
	450–470	C _k	0.715286 ± 10	146.9	n.d.	58.7	n.d.	n.d.	n.d.	n.d.	n.d.
PIG	0–5	A _h	0.731436 ± 10	79.0	2340	69.0	0.0338	n.d.	n.d.	n.d.	n.d.
	10–25	E	0.731957 ± 12	73.3	2067	63.3	0.0355	n.d.	n.d.	n.d.	n.d.
	55–75	B _{21t}	0.731480 ± 12	75.1	2071	77.3	0.0363	n.d.	0.36	14	0.0248
	175–200	B _{31t}	0.725876 ± 9	80.4	3253	74.4	0.0247	n.d.	1.22	365	0.0033
	360–380	C _k	0.718701 ± 9	122.1	n.d.	65.4	n.d.	n.d.	n.d.	n.d.	n.d.
	360–380	C _k >2mm ^(c)	0.712154 ± 10	n.d.	n.d.	n.d.	n.d.	n.d.	n.d.	n.d.	n.d.

^a0.5 M CH₃COOH leachate (partial dissolution).

^bHF digest of the silicate after decarbonation with 2.5 M HCl.

^cCalcareous concretions.

^dn.d. = not determined.

several K-bearing minerals in the upper soil horizons (illite, muscovite; Table 6 and Figure 2) support this hypothesis. Moreover, Bullen *et al.* (1997) have argued that during K-feldspar dissolution, Sr is released at a rate that is considerably faster than the overall dissolution rate. They have suggested that, as impurities not perfectly accommodated in the microcline and orthoclase structure, ^{87}Sr and Rb are concentrated at crystal defects and dislocations and that these defects tend to weather more easily, resulting in the preferential release of ^{87}Sr . Consequently, Sr can be leached from the lattice of chemically resistant K-feldspar with little corresponding mass loss of other cations (Åberg *et al.*, 1989; Bullen *et al.*, 1997). The preferential leaching of radiogenic Sr out of the lattice of K-feldspar and

other K-bearing-minerals (muscovite and illitic clays) in the upper soil horizons of the soils studied is therefore believed to be a valid hypothesis. The evolution of the Sr isotopic ratio of the clay fraction is discussed in the next paragraph.

Rb-Sr isotope systematics

Rb-Sr isotope systematics is another useful tool to decipher the soil forming processes. The Rb-Sr isochron diagram, which plots the measured $^{87}\text{Sr}/^{86}\text{Sr}$ ratios against their $^{87}\text{Rb}/^{86}\text{Sr}$ ratios, is a common tool in geochronology for rock dating (Faure, 1986). In contrast to a well-correlated isochron line, which allows calculation of the age of a suite of rocks from the

Table 7 Continued

Location	Sampling depth /cm	Horizon	1 M CH ₃ COONH ₄ extracted				Soil solution			
			⁸⁷ Sr/ ⁸⁶ Sr ± 2σ × 10 ⁻⁶	Sr /mg kg ⁻¹	Ca	Sr/Ca /g g ⁻¹	⁸⁷ Sr/ ⁸⁶ Sr ± 2σ × 10 ⁻⁶	Sr /μg l ⁻¹	Ca	Sr/Ca /g g ⁻¹
MES I	0–5	A _h	0.711725 ± 11	1.10	283	0.0039				
	10–25	E	0.713040 ± 11	0.23	65	0.0036				
	55–75	B _{21t}	0.713321 ± 13	1.44	267	0.0054				
	175–200	B _{31t}	0.712344 ± 13	5.00	1017	0.0050				
MES II	0–5	A _h	0.712138 ± 6	0.89	190	0.0047	0.711225 ± 5	18.61	5076	0.0037
	10–25	E	0.712888 ± 7	0.12	19	0.0062	0.711881 ± 6	12.41	2475	0.0050
	55–75	B _{21t}	0.715291 ± 6	0.48	66	0.0073	0.712286 ± 5	27.33	4691	0.0058
	100–120	B _{22t}	n.d. ^a	6.40	1165	0.0055				
	140–160	B _{31t}	n.d.	5.85	1206	0.0049				
	175–200	B _{31t}	0.712234 ± 7	5.29	1110	0.0048				
	210–220	C	n.d.	5.07	1684	0.0030				
	220–230	C	n.d.	5.10	1633	0.0031				
	230–240	C	0.710707 ± 14	4.60	2068	0.0022				
TUM	0–5	A _h	0.713133 ± 7	0.41	53	0.0079				
	10–25	E	0.712627 ± 9	0.08	21	0.0037				
	55–75	B _{21t}	0.712882 ± 9	2.03	322	0.0063				
	175–200	B _{31t}	0.711844 ± 7	4.90	966	0.0051				
REL II	0–5	A _h	n.d.	0.88	138	0.0064				
	10–25	E	n.d.	0.10	20	0.0050				
	55–75	B _{21t}	n.d.	1.40	183	0.0077				
	175–200	B _{31t}	n.d.	4.34	900	0.0048				
PIG	0–5	A _h	0.711518 ± 8	0.85	276	0.0031				
	10–25	E	n.d.	0.15	40	0.0038				
	55–75	B _{21t}	0.713198 ± 6	1.76	307	0.0057				
	175–200	B _{31t}	0.712607 ± 70	4.95	1273	0.0039				

^an.d. = not determined.

slope of the isochron line, a linear array drawn through the isotope data of a suite of soil horizons might not have any chronological meaning at all. This pseudo-isochron line reflects a simple binary mixing between two end-members, i.e. two originally distinct parent materials (Brass, 1975; Faure, 1986). The Rb-Sr diagram plotted for the sequence of horizons (from the unweathered parent material to the uppermost organic horizons) of five acid leached soils clearly did not show linear arrays. Each profile had a characteristic loop pattern (Figure 5 a). Due to the effects of differential weathering and preferential leaching processes, the proportions of minerals and of trace elements in mineral lattices change throughout the soil profile. Weathering and subsequent leaching affect the Sr isotopic composition and the Rb and Sr contents of each horizon, determining the pattern of the Rb-Sr diagram (Brass, 1975).

The sequence of weathering processes which, step by step, progress from the calcareous loess to the humic layers (see discussion above) are clearly illustrated by the Rb-Sr diagram (Figure 5): (i) from the C_k to the B_{31t} horizon, the dissolution of carbonates (which have a low Sr isotopic ratio and small Rb contents) and the first step of the preferential weathering

of Ca-plagioclase are prevalent in determining a concomitant increase of the ⁸⁷Sr/⁸⁶Sr and the ⁸⁷Rb/⁸⁶Sr ratios (the same trend is observed for C_k horizons experimentally decarbonated with HCl in laboratory) (Table 7); (ii) from the B_{31t} to the B_{21t} horizon (illuvial soil compartment), the preferential weathering of Ca-plagioclase has taken place, as attested by the increase of both ⁸⁷Sr/⁸⁶Sr and ⁸⁷Rb/⁸⁶Sr ratios, due to a relative accumulation of more resistant, radiogenic and Rb-rich minerals; (iii) the weathering of the K-bearing minerals, coupled with a preferential leaching of radiogenic Sr, leads to decreases in the radiogenic to non-radiogenic minerals ratio in the eluvial soil compartment (E horizon), thus lowering the ⁸⁷Rb/⁸⁶Sr ratio and, to a lesser extent, the ⁸⁷Sr/⁸⁶Sr ratio; and (iv) in the uppermost, organic-rich and more strongly acid A_h horizons the decrease of the ⁸⁷Sr/⁸⁶Sr and the increase of the ⁸⁷Rb/⁸⁶Sr ratios can be viewed as the result of an incongruent weathering process that determines the preferential leaching of common and radiogenic Sr versus Rb, which is more tightly bonded to the mineral lattices (Bullen *et al.*, 1997).

The clay fraction had a much larger ⁸⁷Rb/⁸⁶Sr ratio than the silt fraction and the bulk soil; this ratio increased from the C_k

Table 8 Ca and Sr concentrations and Sr/Ca mass ratios of the labile fraction (1 M CH₃COONH₄ extracted) and of the organic matter in the A_h horizon ($\mu\text{g g}^{-1}$ of air dried soil) of the four sites studied. Proportions of Ca and Sr in the bulk soil are also indicated (weight). Numbers III to VI correspond to soil replicates sampled in the MES forest site

Sample Profile	O.M. ^a			Labile fraction ^b			O.M. + Labile fraction ^c			(O.M. + labile)/Bulk soil			Labile/(Labile + O.M.)		
	/wt. %	Ca $\mu\text{g g}^{-1}$	Sr $\mu\text{g g}^{-1}$	Ca $\mu\text{g g}^{-1}$	Sr/Ca $\mu\text{g g}^{-1}$	Sr $\mu\text{g g}^{-1}$	Ca $\mu\text{g g}^{-1}$	Sr/Ca $\mu\text{g g}^{-1}$	Sr $\mu\text{g g}^{-1}$	Ca %	Sr %	Ca %	Sr %	Ca %	Sr %
MES I	18.0	283.1	1.10	0.0039	0.0054	1.25	231.6	0.0054	1.7	9.3	1.7	>100	>100	>100	88.0
MES II	18.2	253.2	1.43	0.0056	0.0072	1.76	245.4	0.0072	2.2	12.1	2.2	>100	>100	>100	80.8
MES III	31.8	166.6	1.23	0.0074	0.0089	2.11	237.1	0.0089	2.9	9.5	2.9	70.3	70.3	70.3	58.0
MES IV	16.7	271.9	0.81	0.0030	0.0036	0.83	231.2	0.0036	1.1	11.4	1.1	>100	>100	>100	97.8
MES V	14.7	141.9	0.83	0.0059	0.0089	0.99	111.7	0.0089	1.3	5.5	1.3	>100	>100	>100	84.1
MES VI	25.9	295.6	1.49	0.0050	0.0060	1.94	325.3	0.0060	2.5	16.0	2.5	90.9	90.9	90.9	76.8
Mean \pm S.D.	21 \pm 7	235 \pm 65	1.1 \pm 0.3	0.0051 \pm 0.0015	0.0067 \pm 0.0021	1.5 \pm 0.5	230 \pm 68	0.0067 \pm 0.0021	1.9 \pm 0.7	10.6 \pm 3.5	1.9 \pm 0.7	105 \pm 22	105 \pm 22	105 \pm 22	81 \pm 13
PIG	17.0	275.8	0.85	0.0031	0.0047	1.17	246.8	0.0047	1.5	10.5	1.5	>100	>100	>100	73.2
TUM	25.2	52.8	0.41	0.0079	0.0125	1.16	92.7	0.0125	1.3	6.0	1.3	56.9	56.9	56.9	35.9
REL II	18.2	130.5	0.65	0.0050	0.0080	1.12	140.5	0.0080	1.4	6.9	1.4	92.9	92.9	92.9	58.3

^aDetermined by the mass difference after calcination at 450°C.

^b1 M CH₃COONH₄ pH 7 extracted.

^c450°C calcination followed by dissolution of ash in 0.1 M HCl.

O.M. for organic matter.

S.D. for standard deviation.

horizon to the overlying B_t and E soil horizons (Figure 5b). This also explains the shift of the silt curve to smaller ⁸⁷Rb/⁸⁶Sr ratios (step 3 above) compared with those of the bulk soil that was influenced by 10–20% of a K- and Rb-rich clay content (Figures 4b and 5a, Tables 7 and 9). The addition of Rb- and ⁸⁷Sr-rich illitic minerals to the < 2 μm soil fraction by physical breakdown of silt-size muscovite explains the increase of both ⁸⁷Rb/⁸⁶Sr and ⁸⁷Sr/⁸⁶Sr ratios in this sequence of horizons. In the clay fraction of the A_h horizon, the evolution of the ⁸⁷Rb/⁸⁶Sr and ⁸⁷Sr/⁸⁶Sr ratios was clearly the same as in the bulk soil and can also be explained by a non-congruent weathering process of illitic clay minerals.

Isotopic markers of exchange processes: ⁸⁷Sr/⁸⁶Sr ratios of the labile soil fraction, the 0.1 M HCl extracts and the soil solution

The 'labile' cation pool is usually viewed as a mixture of cations derived from mineral weathering, atmospheric deposition and, in surface horizons, organic restitution (Capo *et al.*, 1998). In soils, the distribution with depth of the labile Sr depends on factors such as reactive mineral proportions and compositions, mineral weathering rates, atmospheric inputs, extent of biological cycling, efficiency of exchange and downward transport of Sr (Bullen *et al.*, 1997). The isotopic ratio of Sr released by weathering rarely reflects the bulk soil value, being frequently influenced by the selective dissolution of Ca and Sr-rich minerals with a low ⁸⁷Sr/⁸⁶Sr ratio (Bullen *et al.*, 1997; Blum & Erel, 1997). The soils studied support the concept of selective dissolution in that all the Sr isotope ratios of the CH₃COONH₄ extracts are smaller (< 0.7153) than those of the total digests of the bulk soil (> 0.7256) (Table 7).

The ⁸⁷Sr/⁸⁶Sr ratios of the labile pool and of the 0.1 M HCl extracts, which are considered to simulate natural release by selective dissolution of the most weatherable minerals (Miller *et al.*, 1993; Blum *et al.*, 2002; Bullen & Bailey, 2005), cover a nearly similar range throughout the soil profile (Table 7, Figure 6). This suggests that the isotopic composition of the labile fraction is more closely dependent on weathering processes than on external cationic contributions through atmospheric deposition and restitutions from vegetation. The input to the soil exchangeable pool of Sr from atmospheric sources or biological cycling does not appear to impart a dominant control on the soil exchangeable strontium isotopic composition of most of the soil horizons. However, trends with depth of ⁸⁷Sr/⁸⁶Sr ratios of the labile and acid-extractable fractions were not identical and Sr isotopic ratios of the labile pool were sometimes smaller and sometimes larger than those of the HCl extracts (Figure 6). Smaller ⁸⁷Sr/⁸⁶Sr ratios in the labile soil fraction were measured in both the humic layers and the lower part of the illuvial B_t horizon. This can be explained by a larger contribution to the exchangeable cation pool of non-radiogenic Sr sources, distinct from the plagioclase weathering source. Sr input from atmospheric deposition and from

Table 9 $^{87}\text{Sr}/^{86}\text{Sr}$ ratios ($\pm 2\sigma \times 10^{-6}$), Rb, Ca and Sr concentrations and Sr/Ca mass ratios in the silt and clay separates of the MES I soil profile

Location	Sampling depth/cm	Horizon	Silt fraction (2–50 μm)				Clay fraction (<2 μm)					
			$^{87}\text{Sr}/^{86}\text{Sr} \pm 2\sigma \times 10^{-6}$	Sr /mg kg $^{-1}$	Ca /mg kg $^{-1}$	Rb /mg kg $^{-1}$	Sr/Ca /g g $^{-1}$	$^{87}\text{Sr}/^{86}\text{Sr} \pm 2\sigma \times 10^{-6}$	Sr /mg kg $^{-1}$	Ca /mg kg $^{-1}$	Rb /mg kg $^{-1}$	Sr/Ca /g g $^{-1}$
MES I	0–5	A _h	0.731668 \pm 13	81.5	2858	55.5	0.0285	0.729471 \pm 9	56.2	2965	172.1	0.0190
	10–25	E	0.732541 \pm 8	79.2	3001	55.8	0.0264	0.732759 \pm 10	63.3	5280	176.3	0.0120
	55–75	B _{21t}	0.732917 \pm 10	74.0	3402	63.8	0.0218	0.733013 \pm 9	50.0	6328	147.0	0.0079
	175–200	B _{31t}	0.728157 \pm 10	83.6	4531	66.9	0.0185	0.731419 \pm 11	56.0	1358	141.1	0.0413
	300–320	C _k ^(a)	0.725548 \pm 10	84.3	5666	59.7	0.0149	0.728492 \pm 9	62.3	786	146.5	0.0793

^aHF digest of the silicate residue after progressive carbonate dissolution at pH >5 with 0.1 M HCl.

organic restitutions ($^{87}\text{Sr}/^{86}\text{Sr}$ ratios are 0.7091 and 0.7112, respectively), can be put forward to justify small Sr isotopic ratios of the labile soil fraction in the uppermost and organic-rich horizons of the soil profiles (0.7121 ± 0.0007 ; mean \pm SD; $n = 4$). In soils developed on granitic parent materials, Blum & Erel (1997) had already concluded that there were no appreciable atmospheric contributions of Sr to the soil cation exchangeable pool at soil depths greater than about 10 cm. In the MES forest site, calculation of the two sources contributing to the labile Sr pool of the A_h horizon, using the mixing equations (Equations 1 and 2), shows that the Sr and Ca contributions from the atmospheric source are $33 \pm 16\%$ and $16 \pm 9\%$, respectively ($n = 4$).

The Sr isotopic values of the laboratory 0.1 M HCl soil leaching measured in the lower part of the illuvial soil compartment (B_{31t} horizon ~ 0.7136 ; Table 7), were significantly larger than those of the CH₃COONH₄ extracts (0.7122). Those data suggest that the soil exchange complex at this depth (~ 180 cm) has been supplied by a source of Sr (and, by inference, of Ca) clearly distinct from the weathering source. At such depth, this source cannot be attributed to organic res-

titutions or atmospheric deposition. Our view is that the exchangeable pool of the B_{31t} horizon was partly saturated by Sr cations coming from the previous dissolution of carbonate minerals, currently removed from this horizon, but present in the unweathered loess (C_k horizon, at around 300 cm depth, with a CaCO₃ content of $\sim 13\%$). The calculation of the proportion of the two putative sources of labile Sr using the mixing equations shows that Sr and Ca inherited from carbonates represent a significant proportion of the exchangeable pool in the B_{31t} horizon ($24 \pm 6\%$ for Sr; $7 \pm 2\%$ for Ca; mean \pm SD, $n = 4$). In these soil horizons the exchangeable pool is obviously not representative of present-day weathering processes and contains a more or less important residual pool of Sr.

In contrast to the situation at 180 cm depth, in the middle part of the illuvial soil compartment (B_{21t} horizon; ~ 60 cm depth), the Sr isotopic ratio is clearly greater in the labile pool (0.7137 ± 0.0007 , $n = 3$) than in the 0.1 M HCl soil extract (0.7121, $n = 2$; one value of the CH₃COONH₄ extracts is markedly different from the three other labile replicates and has been discarded). We contend that the exchange complex at this depth is

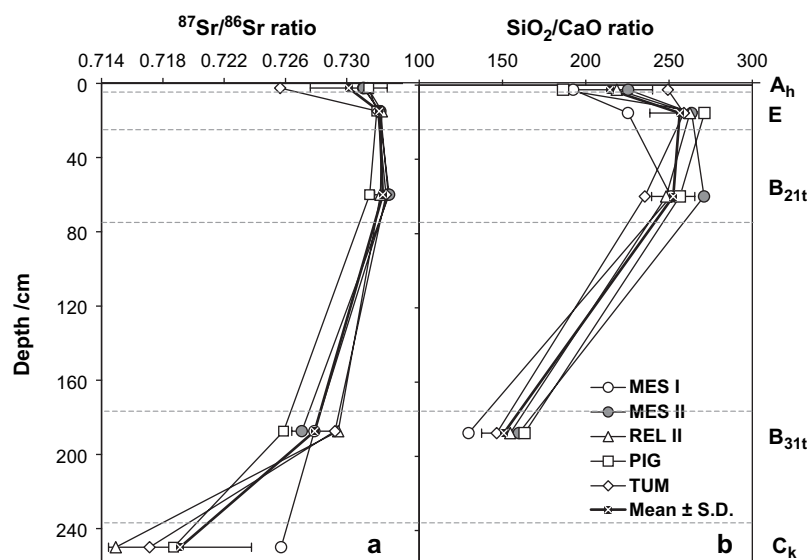
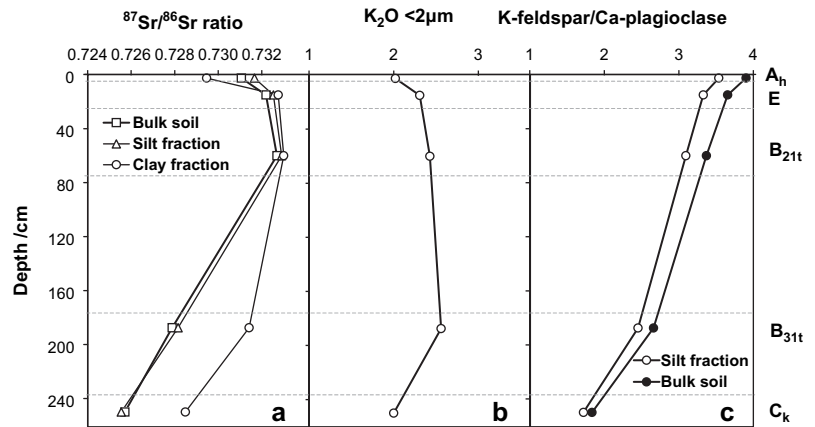


Figure 3 Distribution with depth of (a) the $^{86}\text{Sr}/^{86}\text{Sr}$ ratios of the bulk soil and (b) the SiO_2/CaO molar ratios in the bulk soil of the MES I, MES II, TUM, PIG and REL II soil profiles (error bars show standard deviation).

Figure 4 Distribution with depth of (a) the $^{86}\text{Sr}/^{86}\text{Sr}$ ratios of the bulk soil and of the clay and silt separates, (b) the K_2O content of the clay fraction, and (c) the K-feldspar/Ca-plagioclase mineral ratios in the silt fraction and in the bulk soil in the MES I profile. Analyses of 250-cm depth horizons are made on HCl decarbonated soil samples.



supplied by radiogenic Sr originating from the overlying E and A_h horizons, where the weathering reinforcement of K-bearing minerals generates preferential leaching of radiogenic Sr. Moving downwards, these cations are thought to be held on the more abundant exchange sites of the underlying clay-enriched B_t horizons, which present a greater CEC than the overlying E horizon (Table 1). As a result, the $^{87}\text{Sr}/^{86}\text{Sr}$ ratio of the Sr exchangeable pool was larger than that of the modern weathering source measured by the HCl extract. It is, however, difficult to determine if the current Sr isotopic signature of the exchangeable pool of the illuvial B_{21t} horizon was mainly determined by present-day or former weathering and lixiviation processes. In agreement with Blum & Erel (1997), we hypothesize that the $^{87}\text{Sr}/^{86}\text{Sr}$ ratio of the exchangeable pool is a record of the integrated soil processes (weathering associated in the present case with a downward translocation of cations) over the age of the soil and not a signature of present-day weathering.

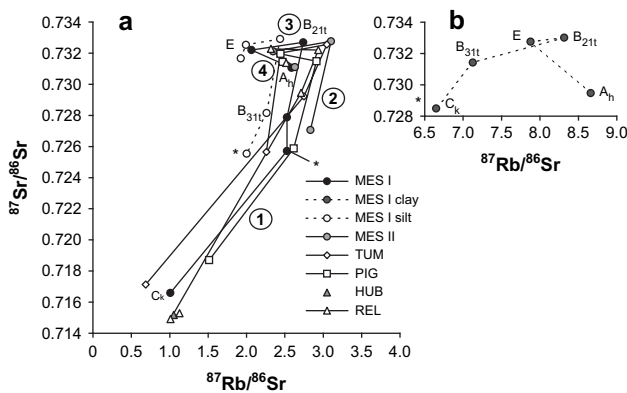


Figure 5 Rb-Sr plot for the parent material and the different horizons of the MES I, MES II, TUM, PIG, REL II and HUB soil profiles. (a) Bulk soil and silt fraction (2–50 μm). The numbers (1, 2, 3, 4) refer to the successive weathering steps (see text for explanation). (b) Clay fraction (< 2 μm) of the MES II soil profile. Asterisk (*) indicates C_k horizons decarbonated by HCl in the laboratory.

The Sr isotopic composition was determined in three soil-water samples collected in the MES site from the A_h , E and B_{21t} horizons using porous tension probes (Table 7). The Sr released in the soil solution is derived from: (i) the dissolution of minerals (depending on the relative weatherability of the strontium containing mineral phases); (ii) the ionic exchange processes between soil colloids and surrounding water; (iii) the flow of gravity water (atmospheric input); and (iv) in the uppermost soil horizons, the mineralization of organic matter. In the MES forest site, the evolution with depth of the Sr isotopic composition of the soil water and of the labile pool was largely similar (Figure 6), confirming cation exchange between the soil exchange sites and the soil solution. However,

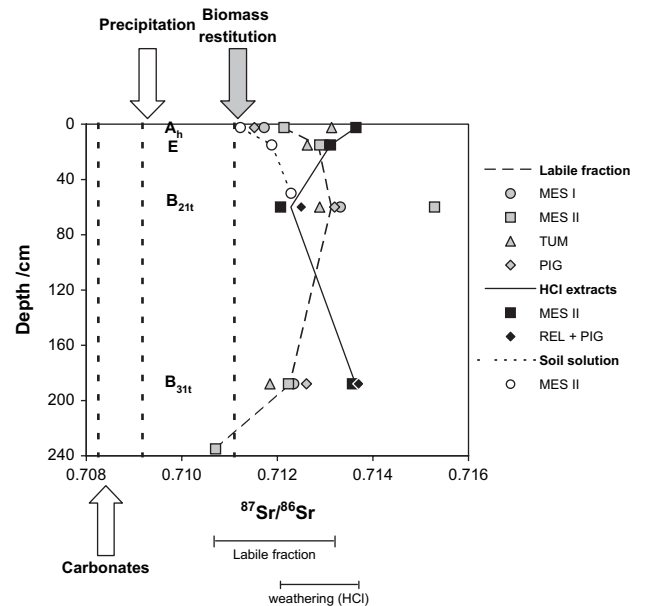


Figure 6 $^{87}\text{Sr}/^{86}\text{Sr}$ ratios of different soil pools (soil water, labile fraction, 0.1 M HCl extracts) in the main soil horizons of the MES, REL II and PIG sites. The Sr isotopic signature of bulk precipitation, biomass returns (beech leaves) and CaCO_3 pools of the MES site are represented by dotted lines.

the $^{87}\text{Sr}/^{86}\text{Sr}$ ratios of the soil solution were smaller than the corresponding ratios of the labile pool, suggesting a contribution from the atmospheric Sr source ($^{87}\text{Sr}/^{86}\text{Sr}$ ratio of the bulk precipitation = 0.709) to the soil water pool. But this also reveals a disequilibrium between the soil solution and the exchangeable cation pool (Bullen *et al.*, 1997; Stewart *et al.*, 1998), which implies that all possible Sr exchange sites are not equilibrated isotopically with the soil waters, in opposition to the common view that the cation exchange between the soil exchange sites and the soil solution is a near-instantaneous process (Davis & Kent, 1990; Johnson & DePaolo, 1994).

Conclusions

Acting as an analogue of Ca, natural strontium isotopes are undeniably powerful tools, as tracers of nutrient sources of forest stands and as monitors of weathering processes in soils and catchments. In the present study, the Sr isotopic method is mainly used in a 'soil genesis' perspective, with special insights into the soil forming processes that characterize the acid leached soils developed under beech forest on a loessic parent material. The determination of the Sr isotopic composition of different soil pools (bulk soil, labile pool, HCl extracts simulating weathering, soil solution) was therefore applied in conjunction with physico-chemical investigations and a mineralogical assessment method. The coupling of these two methods highlights a sequence of weathering processes that progresses from the calcareous loess to the humic layers: (i) from the C_k to the B_{311} horizon, dissolution of carbonates and first step of the preferential weathering of Ca-plagioclase; (ii) from the B_{311} to the B_{211} horizon, preferential weathering of Ca-plagioclase; (iii) in the eluvial soil compartment (E horizon), weathering of the K-bearing minerals, coupled with a preferential leaching of radiogenic Sr; and (iv) in the uppermost, organic-rich and more strongly acid A_h horizon, incongruent weathering processes of K-feldspar. Natural Sr isotopes also provide a better understanding of exchange processes and biological cycling and especially of the origin of the soil exchangeable fraction. In some soil horizons, the systematic Sr isotopic differences between the labile pool and the 0.1 M HCl extracts, which simulate natural weathering, confirm the hypothesis that the $^{87}\text{Sr}/^{86}\text{Sr}$ ratio of the exchangeable pool is a record of the integrated soil processes (weathering associated with a downward translocation of cations or remaining of CaCO_3 dissolution) over the age of the soil and not a signature of present-day weathering. External cationic contributions through atmospheric deposition and restitutions from vegetation is very limited and confined to the top horizon.

Finally, Sr isotopes also reveal a disequilibrium between the soil solution and the exchangeable cation pool, which implies that all possible Sr exchange sites are not equilibrated isotopically with the soil waters, in opposition to the common view that the cation exchange between the soil exchange sites and the soil solution is a near-instantaneous process.

Acknowledgements

We gratefully acknowledge A. Bernard (ULB) for the X-ray diffraction analyses of minerals, and G. Bologne (Université de Liège) for the XRF measurements. Patricia Hermand is warmly thanked for the maintenance of the mass spectrometer and the supervision of the isotopic measurements. We are grateful to two anonymous referees for their critical comments. Financial support was provided by the Fonds National de la Recherche Scientifique (FNRS, Belgium) through the convention FRFC nr 2.4570.02F and by the Fonds pour la formation à la Recherche dans l'Industrie et l'Agriculture (FRIA, Belgium).

References

- Åberg, G., Jacks, G. & Hamilton, P.J. 1989. Weathering rates and $^{87}\text{Sr}/^{86}\text{Sr}$ ratios: an isotopic approach. *Journal of Hydrology*, **109**, 65–78.
- Ashwal, L.D., Demaiffe, D. & Torsvik, T.H. 2002. Petrogenesis of Neoproterozoic granitoids and related rocks from the Seychelles: the case for an Andean-type arc origin. *Journal of Petrology*, **43**, 45–83.
- Bailey, S.W., Hornbeck, J.W., Driscoll, C.T. & Gaudette, H.E. 1996. Calcium inputs and transport in a base-poor forest ecosystem as interpreted by Sr isotopes. *Water Resources Research*, **32**, 707–719.
- Bain, D.C. & Bacon, J.R. 1994. Strontium isotopes as indicators of mineral weathering in catchments. *Catena*, **22**, 201–214.
- Blum, J.D. & Erel, Y. 1997. Rb-Sr isotope systematics of a granitic soil chronosequence: the importance of biotite weathering. *Geochimica et Cosmochimica Acta*, **61**, 3193–3204.
- Blum, J.D., Klaue, A., Nezat, C.A., Driscoll, C.T., Johnson, C.E., Siccama, T.G. *et al.* 2002. Mycorrhizal weathering of apatite as an important calcium source in base-poor forest ecosystems. *Nature*, **417**, 729–731.
- Bologne, G. & Duchesne, J.C. 1991. Analyse des roches silicatées par spectrométrie de fluorescence X: précision et exactitude. *Belgian Geological Survey Professional Paper*, **249**, 1–11.
- Brahy, V., Deckers, J. & Delvaux, B. 2000. Estimation of soil weathering stage and acid neutralizing capacity in a toposequence Luvisol-Cambisol on loess under deciduous forest in Belgium. *European Journal of Soil Science*, **51**, 1–13.
- Brass, G.W. 1975. The effect of weathering on the distribution of strontium isotopes in weathering profiles. *Geochimica et Cosmochimica Acta*, **39**, 1647–1653.
- Bullen, T.D. & Bailey, S.W. 2005. Identifying calcium sources at an acid deposition-impacted spruce forest: a strontium isotope, alkaline earth element multi-tracer approach. *Biogeochemistry*, **74**, 63–99.
- Bullen, T.D., White, A.E., Blum, A.E., Harden, J.W. & Schulz, M. 1997. Chemical weathering of a soil chronosequence on granitoid alluvium. II. Mineralogic and isotopic constraints on the behavior of strontium. *Geochimica et Cosmochimica Acta*, **61**, 291–306.
- Capo, R.C., Stewart, B.W. & Chadwick, O.A. 1998. Strontium isotopes as tracers of ecosystem processes: theory and methods. *Geoderma*, **82**, 197–225.
- Clow, D.W., Mast, M.A., Bullen, T.D. & Turk, J.T. 1997. Strontium $^{87}\text{Sr}/^{86}\text{Sr}$ as a tracer of mineral weathering reactions and

- calcium sources in an alpine/subalpine watershed, Loch Vale, Colorado. *Water Resources Research*, **33**, 1335–1351.
- Coffman, C.B. & Fanning, D.S. 1974. 'Vermiculite' determination on whole soils by cation exchange capacity methods. *Clay and Clay Minerals*, **22**, 271–283.
- Davis, J.A. & Kent, D.B. 1990. Surface complexation modeling in aqueous geochemistry. In: *Reviews in Mineralogy, Volume 23. Mineral-Water Interface Geochemistry* (eds M.F. Hochella & A.F. White), pp. 177–260. Mineralogical Society of America, Washington DC.
- Drouet, Th, Herbauts, J. & Demaiffe, D. 2005b. Long-term records of strontium isotopic composition in tree rings suggest changes in forest calcium sources in the early 20th century. *Global Change Biology*, **11**, 1926–1940.
- Drouet, Th, Herbauts, J., Gruber, W. & Demaiffe, D. 2005a. Strontium isotope composition as a tracer of calcium sources in two forest ecosystems in Belgium. *Geoderma*, **126**, 203–223.
- Duchaufour, Ph & Souchier, B. 1966. Note sur une méthode d'extraction combinée de l'aluminium et du fer libre dans les sols. *Science du Sol.*, **1**, 17–30.
- El Bayad, J. 1996. *Dégradation hydromorphe des sols limoneux acides sous monoculture de hêtre en Forêt de Soignes*. PhD thesis. Université Libre de Bruxelles, Bruxelles.
- FAO-Unesco 1975. *Carte Mondiale des Sols. I. Légende*. FAO-Unesco, Paris.
- Faure, G. 1986. *Principles of Isotope Geology*, 2nd edn. J. Wiley & Sons, New York.
- Graustein, W.C. & Armstrong, R.L. 1983. The use of strontium-87/strontium-86 ratios to measure atmospheric transport into forested watersheds. *Science*, **219**, 289–292.
- Haesaerts, P. 1985. Les lœss du Pléistocène supérieur en Belgique; comparaisons avec les séquences d'Europe centrale. *Bulletin de l'Association Française pour l'étude du Quaternaire*, **2–3**, 105–115.
- Johnson, T.M. & DePaolo, D.J. 1994. Interpretation of isotopic data in groundwater-rock systems: model development and application to strontium isotope data from Yucca Mountain. *Water Resources Research*, **30**, 1571–1587.
- Kennedy, M.J., Hedin, L.O. & Derry, L.A. 2002. Decoupling of unpolluted temperate forests from rock nutrient sources revealed by natural $^{87}\text{Sr}/^{86}\text{Sr}$ and ^{84}Sr tracer addition. *Proceedings of the National Academy of Science*, **99**, 9639–9644.
- Kiely, P.V. & Jackson, M.L. 1965. Quartz, feldspar and mica determination for soils by sodium pyrosulfate fusion. *Soil Science Society of America Proceedings*, **29**, 159–163.
- Kohut, C.K. & Warren, C.J. 2000. Chlorites. In: *Soil Mineralogy with Environmental Applications* (eds J.B. Dixon & D.G. Schulze), pp. 531–553. SSA Book Series 7. Soil Science Society of America, Madison, Wisconsin.
- Lelong, F. & Souchier, B. 1970. Bilans d'altération dans la séquence de sols vosgiens, sols brun acides à podzols, sur granite. *Bulletin du Service de la Carte Géologique d'Alsace et de Lorraine*, **23**, 113–143.
- Miller, E.K., Blum, J.D. & Friedland, A.J. 1993. Determination of soil exchangeable-cation loss and weathering rates using Sr isotopes. *Nature*, **362**, 438–441.
- Olson, C.G., Thompson, M.L. & Wilson, M.A. 2000. Phyllosilicates. In: *Handbook of Soil Science* (ed. M.E. Sumner), F77-F123. CRC Press, Boca Raton, FL.
- Penninckx, V., Meerts, P., Herbauts, J. & Gruber, W. 1999. Ring width and element concentration in beech (*Fagus sylvatica* L.) from a periurban forest in central Belgium. *Forest Ecology and Management*, **113**, 23–33.
- Poszwa, A., Ferry, B., Dambrine, E., Pollier, B., Wickman, T., Loubet, M. *et al.* 2004. Variations of bioavailable Sr concentration and the $^{87}\text{Sr}/^{86}\text{Sr}$ ratio in boreal forest ecosystems. Role of biocycling, mineral weathering and depth of root uptake. *Biogeochemistry*, **67**, 1–20.
- Probst, A., El Gh'mari, A., Aubert, D., Fritz, B. & McNutt, R. 2000. Strontium as a tracer of weathering processes in a silicate catchment polluted by acid atmospheric inputs, Strengbach, France. *Chemical Geology*, **170**, 203–219.
- Schulze, D.G. 2002. An introduction to soil mineralogy. In: *Soil Mineralogy with Environmental Applications* (eds J.B. Dixon & D.G. Schulze), pp. 1–35. Soil Science Society of America, Madison, Wisconsin.
- Schwertmann, U. 1964. Differenzierung der Eisenoxide des Bodens durch Extraktion mit Ammoniumoxalat-lösung. *Zeitschrift für Pflanzenernährung, Düngung und Bodenkunde*, **105**, 194–202.
- Sohet, K., Herbauts, J. & Gruber, W. 1988. Changes caused by Norway spruce in an ochreous brown earth, assessed by the isoquartz method. *Journal of Soil Science*, **39**, 549–561.
- Stewart, B.W., Capo, R.C. & Chadwick, O.A. 1998. Quantitative strontium isotope models for weathering, pedogenesis and biogeochemical cycling. *Geoderma*, **82**, 173–195.
- Van Ranst, E., De Coninck, F., Tavernier, R. & Langohr, R. 1982. Mineralogy in silty to loamy soils of central and high Belgium in respect to autochthonous and allochthonous materials. *Bulletin de la Société Belge de Géologie*, **91**, 27–44.